Bioorganic Chemistry 91 (2019) 103175

Contents lists available at ScienceDirect

Bioorganic Chemistry

journal homepage: www.elsevier.com/locate/bioorg

Natural neuroprotective alkaloids from *Stephania japonica* (Thunb.) Miers

Jiao Xiao[a], Tingyu Hao[d,e], Gang Chen[a], Junyu Song[a], Bin Lin[b], Wei Li[a,c], Jikai Xu[d,e], Jingyu Liu[d,e], Yue Hou[d,e,*], Ning Li[a,e,*]

[a] School of Traditional Chinese Materia Medica, Shenyang Pharmaceutical University, Shenyang 110016, PR China
[b] School of Pharmaceutical Engineering, Shenyang Pharmaceutical University, Shenyang 110016, PR China
[c] Faculty of Pharmaceutical Sciences, Toho University, Miyama 2-2-1, Funabashi, Chiba 274-8510, Japan
[d] College of Life and Health Sciences, Northeastern University, Shenyang 110004, PR China
[e] State Key Laboratory for Chemistry and Molecular Engineering of Medicinal Resources, Guangxi Normal University, Guilin, PR China

ARTICLE INFO

Keywords:
Stephania japonica
Neuroinflammation
Hasubanan alkaloids
Stroke

ABSTRACT

Modulating inflammatory responses after stroke can prevent brain injury and, therefore, improve neurological outcome. *Stephania japonica* (Thunb.) Miers is a Chinese folk medicine with the function of dispelling the "wind and blockage" in the human body according to the Chinese medicine theory, in which the symptoms of stroke are caused by the "wind and blockage" in the body. In this paper, we for the first time linked *S. japonica* to stroke by clarifying fifteen alkaloidal constituents including five undescribed (**1–5**) ones and screening out six hasubanan type alkaloids (**1–4**, **7**, **15**) that elicited stronger anti-neuroinflammatory activities than the positive drug. Moreover, the total alkaloid fraction (ASJ) with previously undescribed **3** as the main component was subject to the *in vivo* evaluation of the protective effect in the MCAO-induced brain injury. The results showed that ASJ exhibited potent protective effect against brain injury in the MCAO rat model. The results reported in this paper suggested that the hasubanan alkaloids from *S. japonica* would be an important molecular source for discovering novel therapeutic agents for neuroinflammation-related diseases, such as stroke diseases.

1. Introduction

Stroke remains one of the leading causes of death and disability, being the 3rd leading cause of death in women and the 5th leading cause of death in men in the United States [1]. Nearly 80% of stroke cases are characterized as ischemic stroke, which is one of the most frequent causes of injury to the central nervous system (CNS). To be noted, tissue plasminogen activator (tPA) is so far the only FDA-approved drug for acute ischemic stroke. However, due to the limited post-stroke therapeutic time window, many contraindications, and other side-effects, such as the hemorrhagic transformation, the risk of which will increase when given outside of the therapeutic time window, only less than 10% of acute ischemic stroke patients qualify for the administration of tPA [2,3]. Thus, there is an urgent need for new stroke therapeutics with high safety.

The severity of an ischemic stroke largely depends on the extent of spreading neuroinflammation into the penumbra [4]. Post-ischemic inflammation consists of a cascade of ischemia and reperfusion (I/R)-triggered events involving the brain and its vessels, the circulating blood, and lymphoid organs. After ischemic stroke, an inflammatory response is induced within a few hours, activating microglia and astrocytes to produce cytokines, chemoattractants, and chemokines. Though inflammation is a defense mechanism against infection, it can also be a pathogenic mechanism that exacerbates the stroke and thereby the neurological sequelae [5]. Recent studies show that the extent of systemic inflammation before to and at the time of stroke is a key determinant of acute outcome and long-term prognosis [5,6]. Therefore resolution of inflammation is an emerging new strategy to reduce damage following ischemic stroke, and modulating inflammatory responses after stroke can prevent brain injury and, therefore, improve neurological outcome [7]. It was also reported by a very recent study that anti-inflammatory molecules, such as BML-111 (5*S*, 6*R*, 7-trihydroxyheptanoic acid methyl ester), the analog of the endogenous anti-inflammatory lipid mediator lipoxin A_4, could reduce neuroinflammation in stroke and thereby protect brain functions in a rat model of transient middle cerebral artery occlusion (tMCAO) [8].

Stephania japonica (Thunb.) Miers is a slender twining shrub, widely distributed in the southwestern of China. The roots of this plant were commonly used as a Chinese folk medicine with the function of clearing heat, detoxifying, and dispelling the "wind and blockage" in the human

* Corresponding authors at: School of Traditional Chinese Materia Medica, Shenyang Pharmaceutical University, Wenhua Road 103, Shenyang 110016, China, (N. Li). College of Life and Health Sciences, Northeastern University, Shenyang 110004, PR China. (Y. Hou).
E-mail addresses: liningsypharm@163.com (N. Li), houyue@mail.neu.edu.cn (Y. Hou).

https://doi.org/10.1016/j.bioorg.2019.103175
Received 26 June 2019; Received in revised form 30 July 2019; Accepted 31 July 2019
Available online 01 August 2019
0045-2068/

body according to the Chinese medicine theory, in which the symptoms of stroke are caused by the "wind and blockage" in the body, indicating the high potential of *S. japonica* for the stroke therapy. However, the therapeutic effect of *S. japonica* on stroke remains unknown to date. Thus, in this paper, through a systematic chemical research in conjunction the *in vitro* anti-neuroinflammatory assay and the *in vivo* evaluation based on a rat model of MCAO, the anti-neuroinflammatory effect of five previously undescribed (**1–5**) and ten known (**6–15**) alkaloids from *S. japonica* and the *in vivo* protective effects of the total alkaloid fraction (ASJ) from *S. japonica* with the previously undescribed **3** as the main component in the MCAO-induced brain injury were reported.

2. Results and discussion

2.1. The identification of alkaloids

In vitro anti-neuroinflammatory effect assay showed that the dichloromethane (CH_2Cl_2) fraction of the 80% EtOH extraction of the whole herb of *S. japonica* possessed potent inhibitory effect on the production of NO in LPS-activated microglia. Thus, a systematic chemical research was performed, leading to the identification of five previously undescribed (**1–5**) and ten known (**6–15**) alkaloids (Fig. 1).

Compound **1** was obtained as a colorless crystal. A pseudo-molecular ion at $[M+Na]^+$ *m/z*: 592.2159 (calcd 592.2153 for $C_{30}H_{35}NO_{10}Na$) in the HRESIMS suggested the molecule formula of **1** to be $C_{30}H_{35}NO_{10}$, which requires 14 indices of hydrogen deficiency. The characteristic signals of one *ortho*-substituted aromatic protons at δ_H 6.84 (1H, d, J = 8.4 Hz, H-1), 6.52 (1H, d, J = 8.4 Hz, H-2) and three phenyl signals at δ_H 7.26 (1H, s, H-2′), 6.54 (2H, s, H-5′, H-6′) were also observed in low field of ^{1}H NMR spectrum (Table 1). High-field ranges exhibited proton signals of six methoxyl groups [at δ_H 3.89 (3H, s, 4′-OCH_3), 3.86 (3H, s, 3′-OCH_3), 3.74 (3H, s, 4-OCH_3), 3.59 (3H, s, 8-OCH_3), 3.53 (3H, s, 3-OCH_3) and 3.43 (3H, s, 7-OCH_3)] and a N- methyl group [at δ_H 3.07 (3H, s, N-CH_3)]. The remaining signals in ^{1}H NMR spectrum were assigned to three methylene moieties [at δ_H 3.00 (1H, m, H-5a), 2.00 (1H, m, H-5b), 2.95 (1H, m, H-9a), 1.65 (1H, m, H-9b), 2.97 (1H, d, J = 16.9 Hz, H-15a), 2.45 (1H, d, J = 16.9 Hz, H-15b)] and three methenyl groups [at δ_H 5.57 (1H, m, H-6), 3.58 (1H, d, J = 4.2 Hz, H-7), 4.99 (1H, d-like, J = 6.1 Hz, H-10)] according to the HSQC data. Additionally, typical 16-oxohasubanan framework with a hemiacetal ether bridge between C-8 (101.3) and C-10 (76.0) [9] were suggested on the basis of ^{13}C NMR (Table 2) and HMBC spectrum (Fig. 2). The ^{1}H and ^{13}C NMR data of **1** were closely similar to those of stephalonine G [10], while having additional NMR signals ascribable to a methoxyl group at C-4 and a carbonyl at C-16 as determined by the HMBC correlations from δ_H 3.74 (3H, s, 4-OCH_3) to δ_C 148.1 (C-4), δ_H 3.07 (3H, s, N-CH_3) to δ_C 172.9 (C-16).

The coupling constant of H-6/H-7 (4.2 Hz) suggested a *cis* configuration of H-6 and H-7 [10]. And the cross peaks from H-9a (2.95) to H-15b (2.45) observed in the NOESY spectrum indicated that these protons should be oriented on the same side of the pyrrolidine ring. NOESY correlations between H-10 (4.99) to 8-OCH_3 (3.59), from 8-OCH_3 (3.59) to NCH_3 (3.07) and NOE effects between NCH_3 (3.07) and H-7 (3.58) assigned the relative configuration of **1**. Additionally, a single crystal X-ray diffraction of **1** was successfully afforded using Cu Kα radiation (Fig. 3), confirming an unequivocal designation of absolute conformation as 6*S*, 7*S*, 8*R*, 10*R*, 13*R*, 14*S*. Finally, compound **1** was determined to be 6*S*, 7*S*, 8*R*, 10*R*, 13*R*, 14*S* stephalonine L, as shown in Fig. 1.

Compound **2** was isolated as white powder, and its molecular formula was determined as $C_{30}H_{33}NO_8$ by the accurate molecular ion peak at *m/z* 558.2104 $[M+Na]^+$ (calcd 558.2098 for $C_{30}H_{33}NO_8Na$) in HRESIMS. The 1D-NMR data (Tables 1 and 2) of **2** revealed it had a same backbone as **1**, except for the ester moiety at C-6 in **2**. The ester group was assigned to a cinnamoyl moiety as determined by the typical signals at δ_H 7.41–7.48 (5H, m), 7.10 (1H, d, J = 16.1 Hz, H-7′) and 5.64 (1H, d, J = 16.1 Hz, H-8′). From the HMBC correlations between δ_H 5.38 (H-6) and δ_C 165.8 (CO-9′), the binding site of cinnamoyl moiety was confirmed. The coupling constant value ($J_{H6,\ H7}$ = 4.0 Hz) along with NOE effect of H-7/NCH_3 and H-10/NCH_3 suggested that **2** had the same relative configurations as **1**. The experimental ECD spectrum of **2** resembled that of **1** (Fig. 4A). Additionally, its calculated

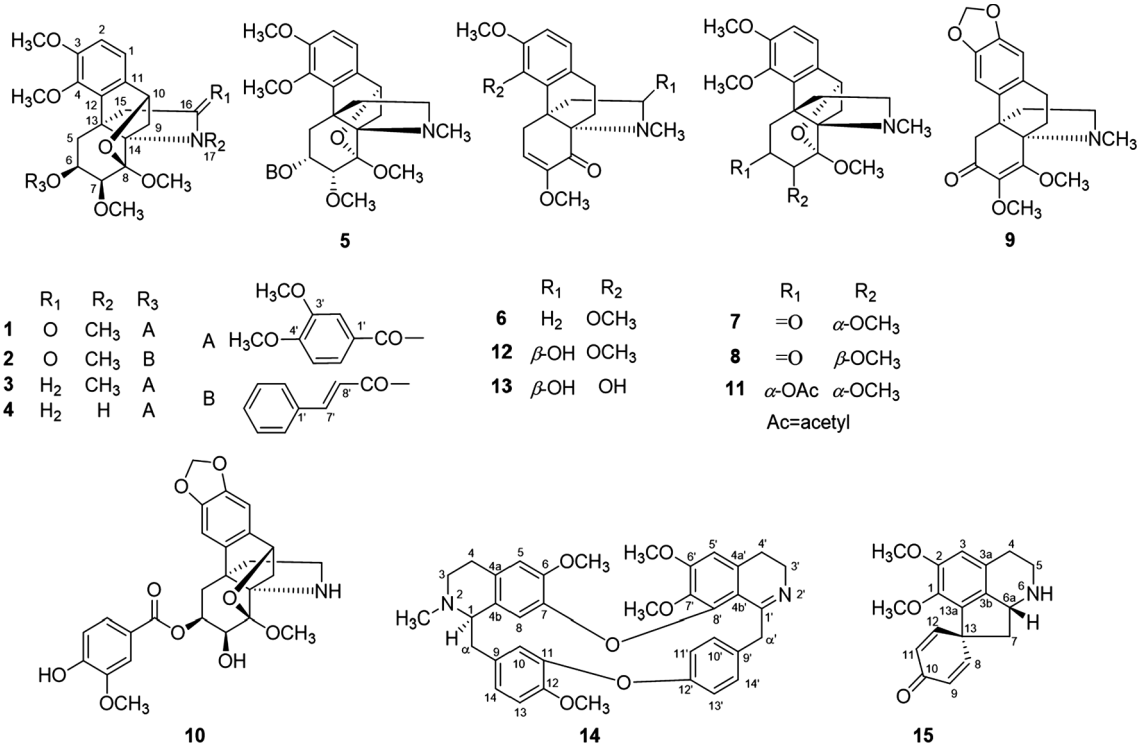

Fig. 1. The structures of identified alkaloids from *S. japonica*.

Table 1
The ^{1}H NMR date for compound **1–5.**

Position	**1**[a]	**2**[b]	**3**[b]	**4**[b]	**5**[b]
	δ_H, multi, (*J* in Hz)				
1	6.84, d (8.4)	6.96, d (8.2)	6.85, d (8.5)	6.80, d (8.1)	6.90, d (8.1)
2	6.52, d (8.4)	6.60, d (8.2)	6.79, d (8.5)	6.76, d (8.1)	6.54, d (8.1)
5a	3.00, m	2.97, m	2.98, m	2.99, m	2.89, m
5b	2.00, m	1.95, m	2.24, m	2.24, m	2.16, m
6	5.57, m	5.38, m	5.52, m	5.47, m	5.38, m
7	3.58, d (4.2)	3.75, d (4.0)	3.89, d (4.6)	3.88, d (4.5)	3.83, d (4.3)
9a	2.95, m	2.97, m	2.73, m	2.52, m	2.71, m
9b	1.65, m	1.81, m	1.62, m	1.93, m	1.61, m
10	4.99, d-like (6.1)	5.08, d-like (6.2)	5.01, d-like (6.1)	4.95, d-like (5.8)	5.00, d-like (6.3)
15a	2.97, d (16.9)	2.87, d (16.9)	2.38, m	2.52, m	2.36, m
15b	2.45, d (16.9)	1.90, d (16.9)	1.90, m	2.00, m	1.90, m
16a			3.41, m	3.18, m	3.39, m
16b			2.62, m	3.18, m	2.57, m
17-NCH$_3$	3.07, s	3.07, s	2.62, s		2.59, s
2′	7.26, s	7.41–7.48, m	7.26, s	7.16, d (1.8)	7.40–7.48, m
3′					
4′					
5′	6.54, s		6.54, s	6.44, d (8.4)	
6′	6.54, s		6.54, s	6.85, dd (8.4, 1.8)	
7′		7.10, d (16.1)			7.10, d (16.1)
8′		5.64, d (16.1)			5.64, d (16.1)
3-OCH$_3$	3.53, s	3.44, s	3.48, s	3.43, s	3.35, s
4-OCH$_3$	3.74, s	3.80, s	3.71, s	3.70, s	3.74, s
7-OCH$_3$	3.43, s	3.75, s	3.45, s	3.40, s	3.41, s
8-OCH$_3$	3.59, s	3.62, s	3.55, s	3.54, s	3.54, s
3′-OCH$_3$	3.86, s		3.86, s	3.84, s	
4′-OCH$_3$	3.89, s		3.89, s	3.87, s	

[a] In $CDCl_3$.
[b] In CD_3OD.

ECD spectrum matched the experimental ECD data perfectly (Fig. 4B), allowing the structure of **2** to be determined as 6*S*, 7*S*, 8*R*, 10*R*, 13*R*, 14*S*-stephalonine M.

Compound **3** was afforded as white powder. Its molecular formula $C_{30}H_{37}NO_9$ was deduced via HREIMS, losing 14-Da molecular weight than that of compound **1**. Detailed comparison of the ^{1}H, ^{13}C NMR (Tables 1 and 2), and 2D NMR data between **3** and **1** indicated that they both had a same hasubanan skeleton, while the carbonyl group (δ_C 172.9, C-16) in **1** was replaced by a methylene group (δ_C 55.2, δ_H 3.41 and 2.62) in **3**. The coupling constant between H-6 and H-7, and NOESY cross-peaks of H-10/H-7 and H-10/NCH$_3$ implied that the aforementioned protons were all α-oriented. Finally, the calculated and experimental ECD spectra (Fig. 4C) demonstrated the structure of **3** as 6*S*, 7*S*, 8*R*, 10*R*, 13*R*, 14*S*- stephalonine N.

Compound **4** was isolated as yellow powder. The 1D NMR spectra of **4** exhibited most of the structural features found in **3**, except for the absence of 17-CH$_3$ in **4**. The absence of 17-CH$_3$ was further confirmed via the HRESIMS data of **4**, exhibiting an $[M+H]^+$ ion peak at *m/z* 542.2390 (calcd 542.2385 for C29H36NO9). Its relative configuration was determined to be 6*S**, 7*S**, 8*R**, 10*R**, 13*R**, 14*S** based on the key coupling constant value ($J_{H\text{-}6,H\text{-}7}$ = 4.5 Hz) and NOESY correlations of H-15b/H-7, H-10/H-7. Calculated ECD curves (Fig. 4C) of (6*S*, 7*S*, 8*R*, 10*R*, 13*R*, 14*S*)-**4** represented high homogeneity with the experimental data, allowing the determination of the absolute configurations of **4**. And compound 4 was elucidated as 6*S*, 7*S*, 8*R*, 10*R*, 13*R*, 14*S*-stephalonine O.

The HRESIMS of **5** (stephalonine P) gave a quasi-molecular ion peak $[M+H]^+$ at *m/z* 522.2492 (calcd. 522.2486 for $C_{30}H_{36}NO_7$), which was 14 Da less than that of **2**. Through analyzing NMR data (Tables 1 and 2) and tracing the continuities in the HMBC and ^{1}H-^{1}HCOSY spectra, we deduced that **5** shared a high level of structural similarity to **2**, with lower degrees of oxidation at C-16. The HMBC correlations from δ_H 2.59 (17-N-CH$_3$) to 55.2 (C-16) determined that C-16 was replaced by a methylene moiety. The relative configuration of **5** was found to be identical to those of **2** via analyzing coupling constant (4.3 Hz) of H6/H7 and comparing NOESY effects of H-10 (δ 5.00)/NCH$_3$ (δ 2.59), H7 (δ 3.89)/NCH$_3$ (δ 2.59). In spite of the same skeleton shared by **5** and **3**, **4**, the experimental ECD curve of **5** showed positive cotton effects at 219–244 nm, being opposite to **3** and **4** (Fig. 4D). Therefore, we deduced that the absolute configuration of **5** was 6*R*, 7*R*, 8*S*, 10*S*, 13*S*, 14*R*, which was further confirmed based on the calculated ECD spectrum of **5**, which was in good agreement with the experimental data by showing two positive cotton effects at 219–244 nm and 280–350 nm, and one negative cotton effect at 244–280 nm (Fig. 4D). Then, compound **5** were determined to be 6*R*, 7*R*, 8*S*, 10*S*, 13*S*, 14*R*- stephalonine P.

The ten known alkaloids, including (13*R*, 14*S*) – 6, 7 – didehydro – 3, 4, 7 – trimethoxy – 17 – methyl – 8 – oxohasubanan (**6**), (7*S*, 8*S*, 10*S*, 13*R*, 14*R*) – epistephamiersine (**7**) [11–13], (7*S*, 8*S*, 10*S*, 13*R*, 14*R*) – stephamiersine (**8**) [11,12,14], (13*R*, 14*S*) – delavayine (**9**) [15], (6*S*, 7*S*, 8*R*, 10*R*, 13*R*, 14*S*) – stephavanine (**10**) [16], (6*R*, 7*R*, 8*S*, 10*S*, 13*S*,

Table 2
The ^{13}C NMR date for compounds **1–5.**

Position	**1**[a]	**2**[b]	**3**[b]	**4**[b]	**5**[b]	Position	**1**[a]	**2**[b]	**3**[b]	**4**[b]	**5**[b]
1	120.2	121.5	121.3	120.6	121.1	17-NCH$_3$	28.2	28.7	28.2		39.2
2	110.2	111.6	110.2	109.7	110.8	1′	122.1	135.8	123.5	121.9	135.9
3	153.2	154.8	154.7	153.3	154.7	2′	112.2	128.0	114.0	112.6	129.2
4	148.1	149.1	149.1	148.1	149.0	3′	148.0	130.0	149.4	147.9	129.9
5	33.7	33.7	34.6	32.2	34.6	4′	152.7	131.4	154.5	153.3	131.3
6	66.2	68.2	69.6	67.7	69.3	5′	109.3	130.0	111.2	110.0	129.9
7	82.1	83.0	83.2	81.2	82.9	6′	124.3	128.0	125.6	124.2	129.2
8	101.3	102.4	104.7	101.6	104.7	7′	165.8	145.4	167.7	166.3	145.1
9	33.0	34.5	30.0	37.1	29.9	8′		118.5			118.8
10	76.0	77.6	78.7	77.6	78.7	9′		168.0			168.1
11	133.7	134.9	136.4	133.8	136.8	3-OCH$_3$	55.5	55.8	56.0	54.5	55.7
12	132.0	133.2	134.9	133.2	134.8	4-OCH$_3$	60.3	60.9	60.7	59.4	60.8
13	43.2	44.7	50.9	46.5	51.0	7-OCH$_3$	57.8	58.0	58.2	56.4	57.9
14	74.6	76.4	77.9	74.7	77.9	8-OCH$_3$	51.9	52.2	51.8	50.8	51.8
15	44.7	36.9	37.0	37.4	36.9	3′-OCH$_3$	55.9		56.7	55.3	
16	172.9	176.5	55.2	41.0	55.2	4′-OCH$_3$	56.0		56.5	55.1	

[a] In $CDCl_3$.
[b] In CD_3OD.

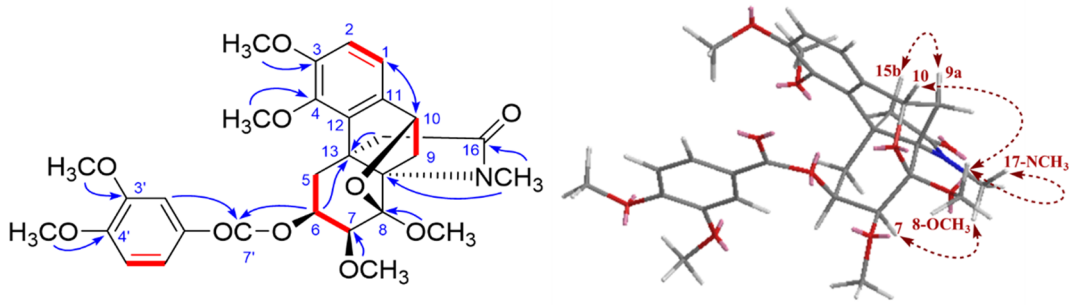

Fig. 2. Key ^{1}H-^{1}H COSY (▬), HMBC (↷), NOESY (↔) correlations of compound **1.**

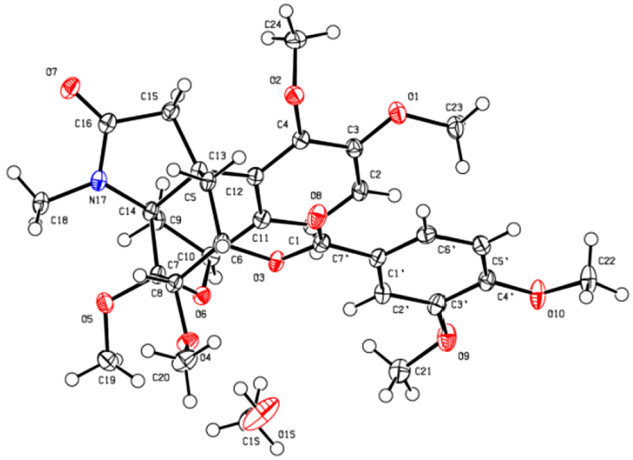

Fig. 3. X-ray (Gu Kα) crystal structure of compound **1.**

14*R*) – 6 – dihydroepistephamiersine – 6 – acetate (**11**), (10*S*, 13*R*, 14*S*) – prometaphanine (**12**) [14], (10*S*, 13*R*, 14*S*) – prostephabyssine (**13**) [13], (1*R*) – epistephanine (**14**) [17,18], and (6a*R*) – stepharine (**15**) [19] were identified as shown (Fig. 1). Among them, compounds **9–11** were not previously reported from this species.

2.2. The anti-neuroinflammatory effects of *1–15* in LPS-treated BV2 cells

Due to the tightly correlated relationship between neuroinflammation and stroke [7,8], the *in vitro* inhibitory effect of all the isolates on NO production by LPS-induced BV2 cells were examined to evaluate their potentials for the therapeutic of stroke. The results showed that the previously undescribed **1–4** and known alkaloids **7**, **15** elicited stronger anti-neuroinflammatory effects than that of the positive drug minocycline (Table 3, Fig. 5), suggesting that alkaloids from *S. japonica* can be ideal natural agents for the treatment of stroke.

2.3. The in vivo protective effect of ASJ in the MCAO-induced brain injury

In order to perform the *in vivo* evaluation of the protective effect of the bioactive **1–4**, **7**, **15**, the attempted enrichment of **1–4**, **7**, **15** was conducted. However, due to the low amount of **1**, **2**, **4**, **7**, and **15**, we finally obtained the total alkaloid fraction (ASJ) containing **3** as the main component (17.9% of the whole ASJ, see Fig. 6A), and subjected the ASJ to the *in vivo* evaluation.

2.3.1. Effects of ASJ on the ischemia-reperfusion injury in MCAO rats

The effect of ASJ on ischemia-reperfusion (I/R) injury was evaluated via testing neurological score, brain water content and infarct volume. The results of the Zea Longa test showed that the neurological score was obviously increased in the MCAO group compared with the control group after reperfusion 0 h ($P < 0.001$, Fig. 6B). Neurological score among MCAO group and ASJ-treated group were similar which indicated that ischemia-reperfusion injury was established successfully and the ischemia-reperfusion injury in different groups were parallel.

Twenty-four hours after reperfusion, neurological score was reduced in the ASJ-treated (200 mg/kg) group ($P < 0.05$, Fig. 6C), which showed a significant neuroprotective effect of ASJ (200 mg/kg) on the MCAO rats. The brain water content was significantly increased in MCAO group compared with the control group ($P < 0.05$, Fig. 6D). Administration of ASJ (200 mg/kg) produced a significant decrease in brain edema compared to the MCAO group ($P < 0.05$). The TTC results showed that MCAO caused significantly infarct volume compared to control group ($P < 0.01$, Fig. 6E and F), which was significantly reduced by ASJ (200 mg/kg) ($P < 0.05$).

The results showed that ASJ (200 mg/kg) administration improved neurological score, decreased the infarct volume and brain water content in the MCAO rat model significantly.

2.3.2. The effect of ASJ on the activation of microglia in MCAO rats

Immunofluorescence testing for Iba-1 was performed to determine microglial response. In terms of cerebral cortex, the results showed that the effect is significant different among different groups. Rats in the MCAO group showed increased number of Iba-1 positive cells compared to the control group ($P < 0.001$, Fig. 7A–C). Administration of ASJ (200 mg/kg) induced a significant decrease in the number of Iba-1 positive cells compared to the MCAO group ($P < 0.001$). Microglia in MCAO group showed shrunk and thickened neurite and enlarged cell body, while microglia in ASJ-treated group showed diminished cell body and normal neurite (Fig. 7B). There is no difference in the number of microglia among all groups in the contralateral brain of surgery (Fig. 7D and E). The results indicated that treatment with ASJ inhibited the activation of microglia, which may contribute to the protective effect of ASJ in MCAO rats.

2.3.3. The effect of ASJ on ischemic neurons in MCAO rats

Immunofluorescence testing for the determination of NeuN, a marker of mature neurons was performed. There was a conspicuous difference in NeuN-stained area of neurons in the rat ischemia cortex among different groups. Rats in the MCAO group showed a significant reduction of NeuN-stained area of neurons in rat ischemia cortex compared to the control group ($P < 0.001$, Fig. 8A and B). Administration of ASJ (200 mg/kg) produced a significant decrease in the number of NeuN-stained area of neurons compared to the MCAO group ($P < 0.001$). There is no obvious difference in the injury of neurons among all groups in the contralateral brain of surgery (Fig. 8C and D). The results suggested that treatment with ASJ diminished neuron damage in MCAO rats and may contribute to anti-stroke effect of ASJ.

3. Conclusion

In this paper, we for the first time linked *S. japonica* to stroke by clarifying fifteen alkaloidal constituents including five undescribed (**1–5**) ones and screening out six components (**1–4**, **7**, **15**) having stronger anti-neuroinflammatory activities than the positive drug. To be

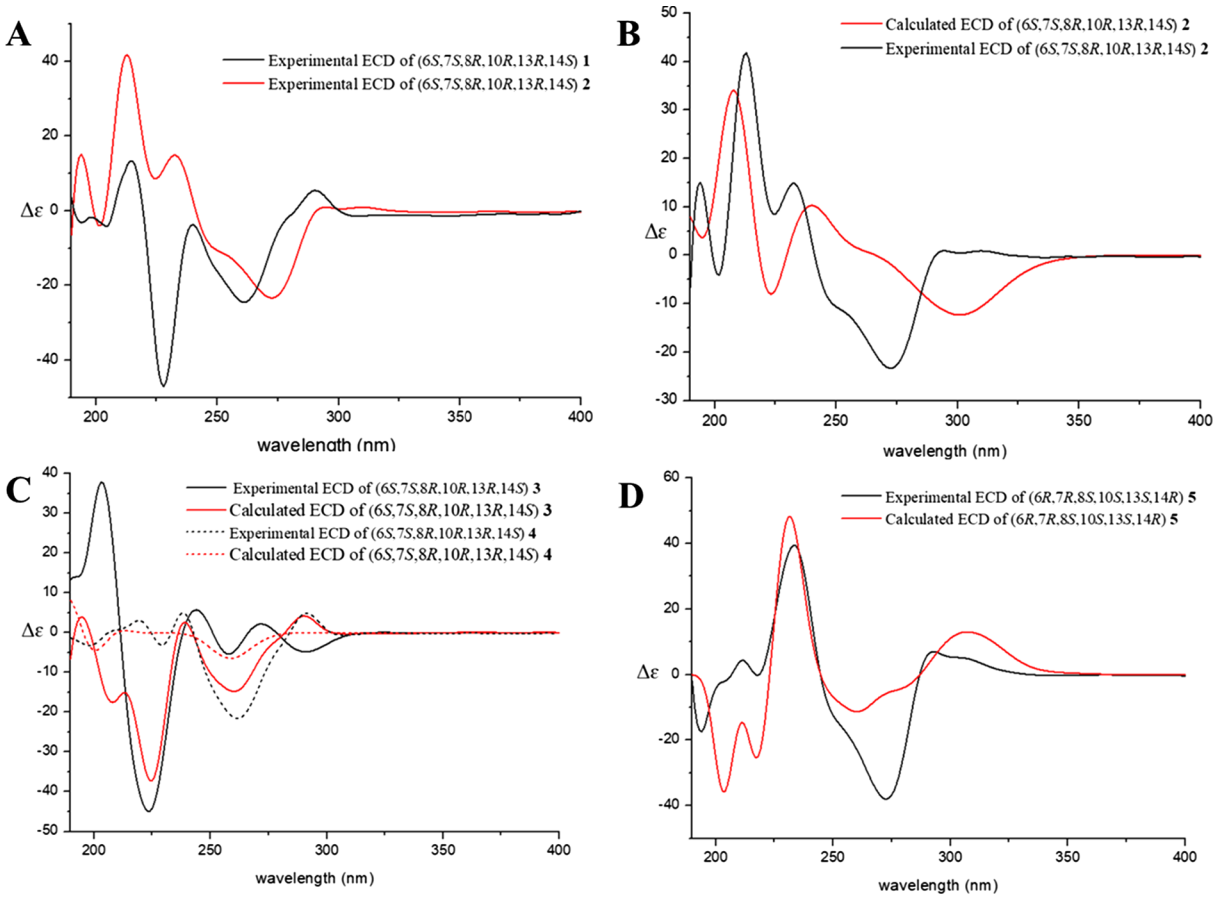

Fig. 4. Calculated and experimental ECD spectra of compounds **1–5**.

Table 3
Effects of extract and pure compounds on NO production by LPS-activated microglia cells.

Compounds	IC_{50} (μM)	Compounds	IC_{50} (μM)
$CHCl_2$ extract	23.85 ± 1.41[a]	**8**	78.13 ± 2.16
ASJ	13.19 ± 1.97[a]	**9**	43.04 ± 1.69
1	1.58 ± 1.26	**10**	> 100
2	0.10 ± 1.02	**11**	> 100
3	13.18 ± 3.19	**12**	> 100
4	1.10 ± 1.96	**13**	> 100
5	34.01 ± 1.52	**14**	17.92 ± 2.23
6	32.67 ± 1.80	**15**	13.91 ± 1.13
7	3.05 ± 1.57	Mino[b]	17.47 ± 3.14

[a] IC_{50} in μg/ml.
[b] Positive control.

noted, all the bioactive **1–4**, **7**, **15** belong to the hasubanan type alkaloids. Furthermore, we prepared the total alkaloid fraction (ASJ) with previously undescribed **3** as the main component, and confirmed the *in vivo* protective effect of ASJ in the MCAO-induced brain injury. As a result, the ASJ containing **3** that accounted for 17.9% of the ASJ elicited potent protective effect by improving neurological score and decreasing the infarct volume and brain water content in the I/R injury of the MCAO rat model. In addition, ASJ also inhibited the activation of microglia and reduced neuronal death. In this study, the main chemical component **3** and other low amount alkaloids (except for **14** and **15**) were all shared the same skeleton of hasubanan alkaloids, indicating that the hasubanan alkaloids from *S. japonica* would be an important molecular source for discovering novel therapeutic agents for neuroinflammation-related diseases, such as stroke diseases.

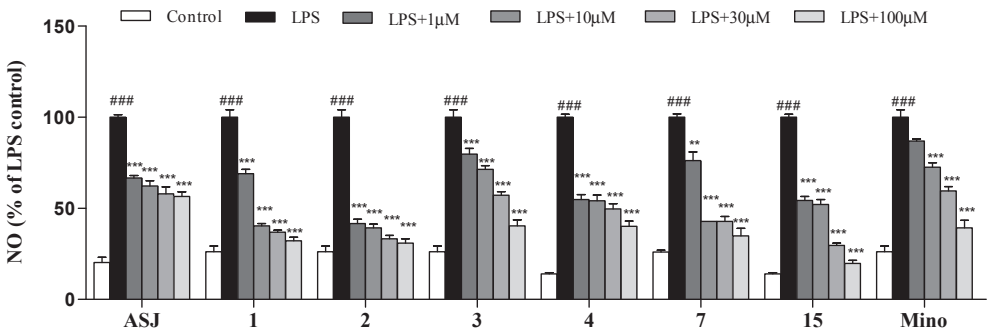

Fig. 5. Anti-inflammatory activities of the ASJ and isolated compounds **1–4**, **7**, **15** assayed on LPS-induced NO production in BV-2 microglial cells. (Each bar represents the mean ± SE of three independent experiments; ###p < 0.001 compared with control group, **p < 0.01, ***p < 0.001 compared with LPS group; ASJ: alkaloidal extract of *S. japonica*, μg/ml, Mino: minocycline).

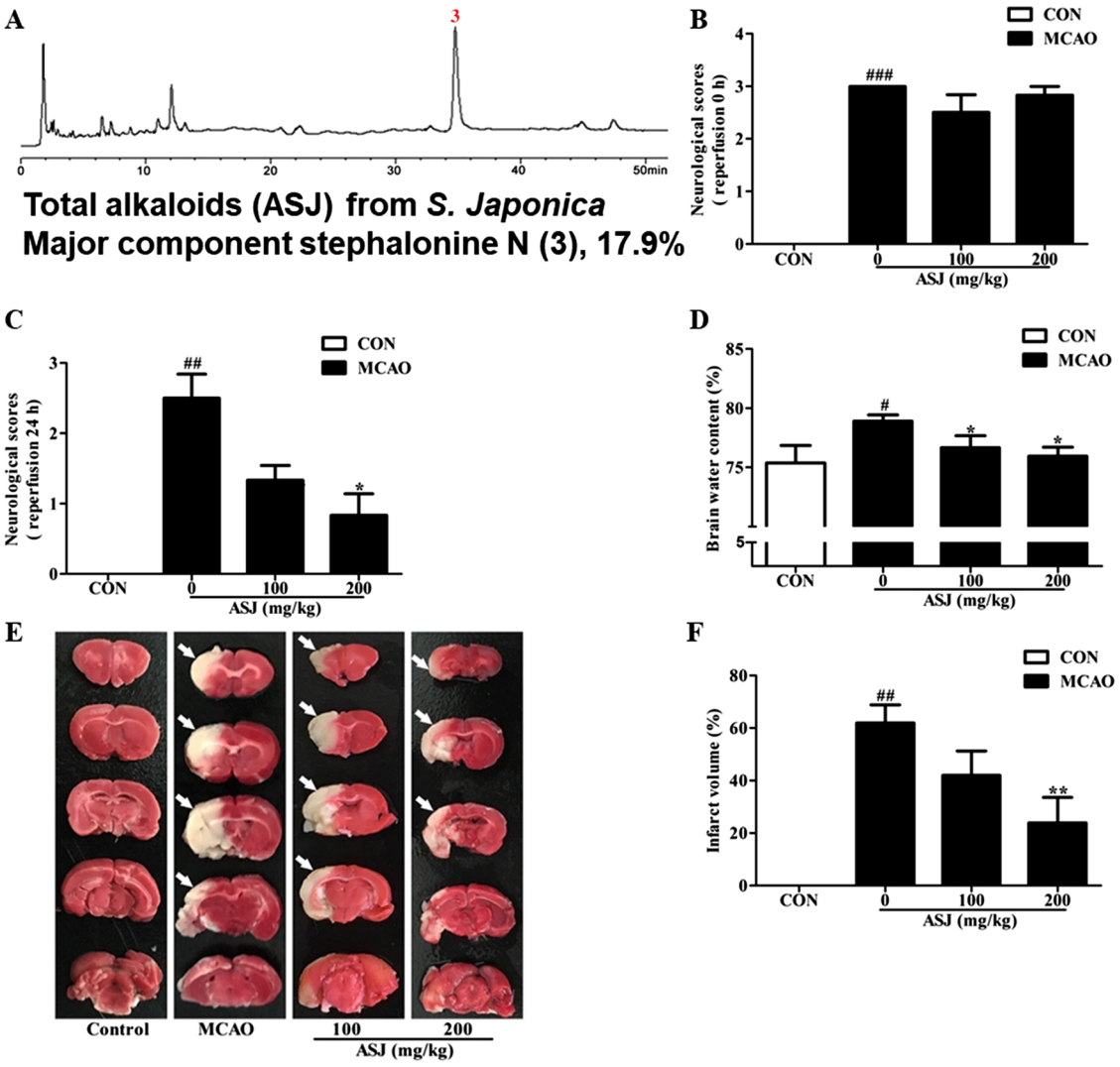

Fig. 6. (A) The HPLC chromatograms of ASJ, compounds **3** was the major chemical constituent of ASJ with the content of 17.9%. (B–F) Effect of ASJ on MCAO rats. Neurological deficit (B and C), cerebral edema (D) and cerebral infarct volume (E and F) were significantly higher in the middle cerebral artery occlusion (MCAO) group compared with the control group. Arrow point to the cerebral infarct segment in (E). The changes induced by MCAO could be significantly reversed by ASJ (200 mg/kg). Values were expressed as Mean ± S.E.M. $\#P < 0.05$, $\#\#P < 0.01$, $\#\#\#P < 0.001$ compared with the control group, $*P < 0.05$, $**P < 0.01$ compared with the MCAO group.

4. Experimental section

4.1. General experimental procedures.

Optical rotations were performed on Perkin-Elmer Model 341 polarimeter. ECD spectra were inscribed on a Bio-Logic Science MOS-450 spectrometer. 1D and 2D-NMR data were recorded on Bruker ARX-400/600 MHz instrument using TMS as an internal standard. Bruker micro-TOFQ-Q mass spectrometer was used to measure HR-ESIMS. Extensive column chromatography (CC) was performed with Macroporous resin HPD-100 (Cangzhou Baoen Chemical Co., Ltd.), silica gel (200–300 mesh, Qingdao Marine Chemical Co. Ltd. China), octadecyl silica (ODS, 50 μm, YMC Co. Ltd., Kyoto, Japan), Sephadex LH-20 (Amersham Pharmacia Biotech AB; SE-715 84 Uppsala Sweden). Preparative HPLC separation was conducted on YMC-PACK ODS-A column (250 × 20 mm, 5 μm) equipped with Shimadzu LC-6AD pump and Shimadzu SPD-20A VP ultraviolet/visible (UV/vis) detector.

4.2. Plant material

The plant material was collected from Hunan province of China in September 2016. Professor Yingni Pan (Shenyang Pharmaceutical University) identified the plant material to be whole herb of *S. japonica*.

4.3. Extraction and isolation

The whole herb of *S. japonica* (9 kg) was immersed and extracted with 80% EtOH (7 × 24 h × 90L). Then, the crude extract (1284.0 g) was suspended in water and partitioned with petroleum ether (PE) to remove chlorophyll, and dichloromethane (CH_2Cl_2) successively to afford the CH_2Cl_2 fraction A1. The aqueous fraction then was alkalic with 4% NaOH to pH 8–9 and further extracted with CH_2Cl_2 (A2), the fractions of A1 and A2 were combined to obtain 100.0 g of total alkaloid fraction (ASJ).

Detailed elution with a step gradient of CH_2Cl_2/MeOH (100:0 to 1:1) on silica gel column chromatography for ASJ fraction gave 9 subfractions (F1–F9). F2 were loaded on HPD-100 macroporous adsorption resins to enrich 70% elution, which was separated to get compounds **1** (75.0 mg), **2** (7.0 mg), **5** (16.9 mg), **6** (2.0 mg), **7** (18.9 mg), **8** (12.3 mg) and **9** (2.5 mg) via ODS column chromatography and preparative HPLC. F3 was subjected to ODS column chromatography eluted with MeOH-H_2O and generate three isolates **3** (11.5 mg),

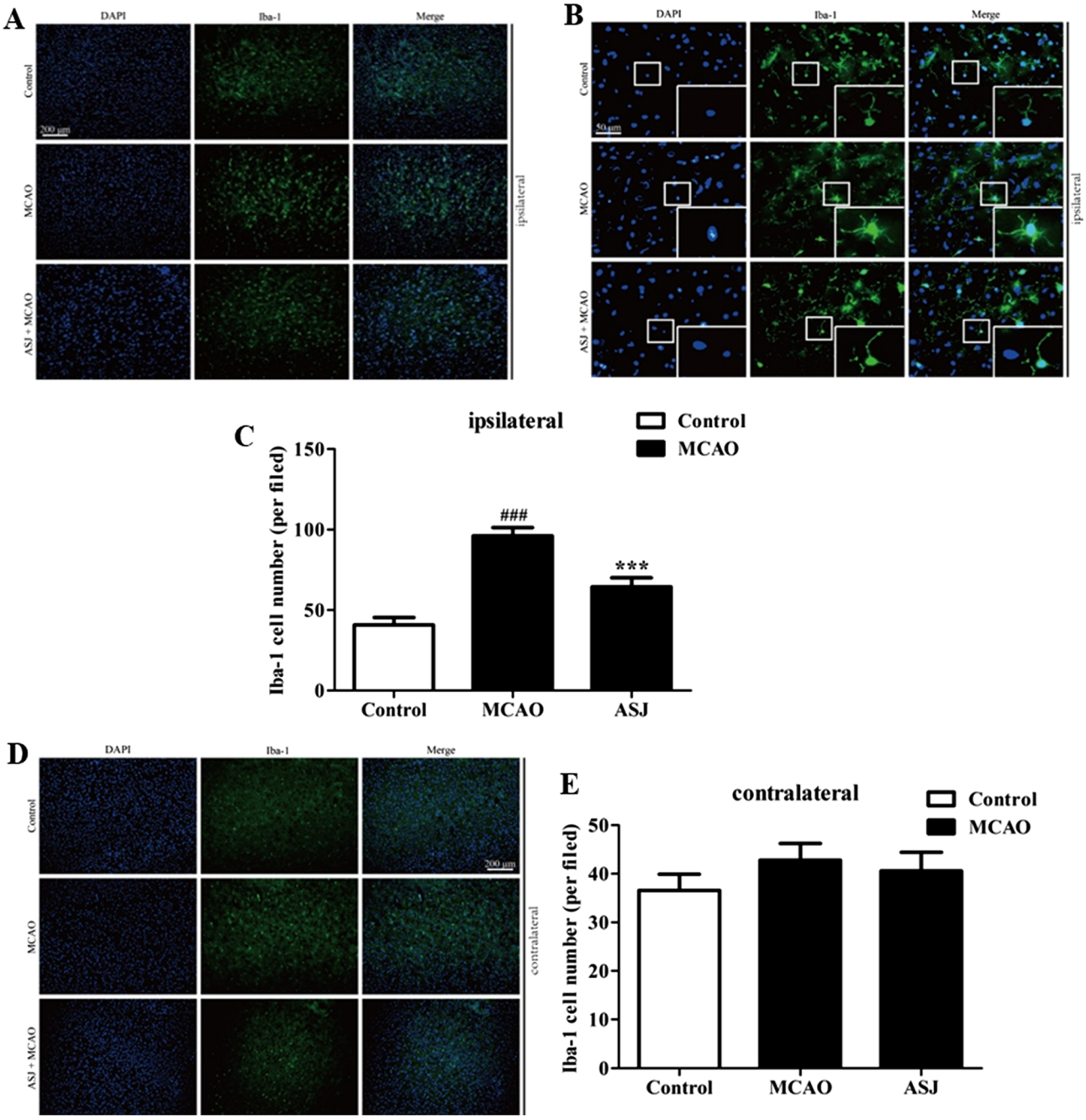

Fig. 7. Effect of ASJ on the number and the morphology of Iba-1 positive cells in ipsilateral (A–C) and contralateral (D and E) cortex of MCAO rats at reperfusion 24 h. Activation of microglia (A–C) could be significantly reversed by ASJ (200 mg/kg). Iba-1 positive cells (green) in the contralateral cortex (D and E) showed no significant difference between the groups. Values were expressed as Mean ± S.E.M, $###p < 0.001$ compared with the control group, $***p < 0.001$ compared with the MCAO group.

11 (12.5 mg) and **12** (2.5 17.0 mg). Compound **4** (3.0 mg) along with **13** (3.0 mg) were obtained from F4 via Sephadex LH-20 column with MeOH. F5 was chromatographed on HPD-100 macroporous adsorption resins column eluting with EtOH-H_2O to give compound **10** (9.0 mg). F6 was chromatographed via silica gel column eluting with PE-EtOAc from 6:1 to 1:1, followed by recrystallization in MeOH to obtain compounds **14** (55.0 mg) and **15** (20.0 mg).

Stephalonine L (**1**), colorless crystal (MeOH); $[\alpha]_D^{20}$ 27.84 (*c* 0.1, MeOH); ECD (MeOH) λ_{max} ($\Delta\varepsilon$) 289.0 (7.51), 259.0 (- 35.50), 225 (−73.57), 237.0 (−4.58); HR-ESI-MS *m/z* $[M+Na]^+$: 592.2159 (calcd. 592.2153 for $C_{30}H_{35}NaNO_{10}$); ^1H and ^{13}C NMR data were showed in Tables 1 and 2.

Stephalonine M (**2**), white powder (MeOH); $[\alpha]_D^{20}$ 62.56 (*c* 0.64, CH_3OH), ECD (MeOH) λ_{max} ($\Delta\varepsilon$) 272.0 (23.33), 294.0 (0.94), 233 (14.82), 225.0 (8.58), 213.0 (41.81), 202.0 (−2.96), 194.0 (15.01); HRESIMS *m/z* $[M+Na]^+$: 558.2104 (calcd. 558.2098 for $C_{30}H_{33}NNaO_8$); ^1H and ^{13}C NMR data were showed in Tables 1 and 2.

Stephalonine N (**3**), white powder (MeOH); $[\alpha]_D^{20}$ – 12.24 (*c* 0.1, CH_3OH); λ_{max} ($\Delta\varepsilon$) 290.0 (4.22), 260.0 (−14.78), 239.0 (2.63), 225.0 (−37.21), 195.0 (3.98), 208.0 (−17.53), 213.0 (−15.06); HRESIMS *m/z* $[M+H]^+$: 556.2547 (calcd. 556.2541 for $C_{30}H_{39}NO_9$); ^1H and ^{13}C NMR data were showed in Tables 1 and 2.

Stephalonine O (**4**), yellow powder (MeOH); $[\alpha]_D^{20}$ – 28.2 (c 0.3 mg/ml, CH_3OH); λ_{max} ($\Delta\varepsilon$) 291.0 (12.21), 262.0 (−53.79), 238.0 (12.54),

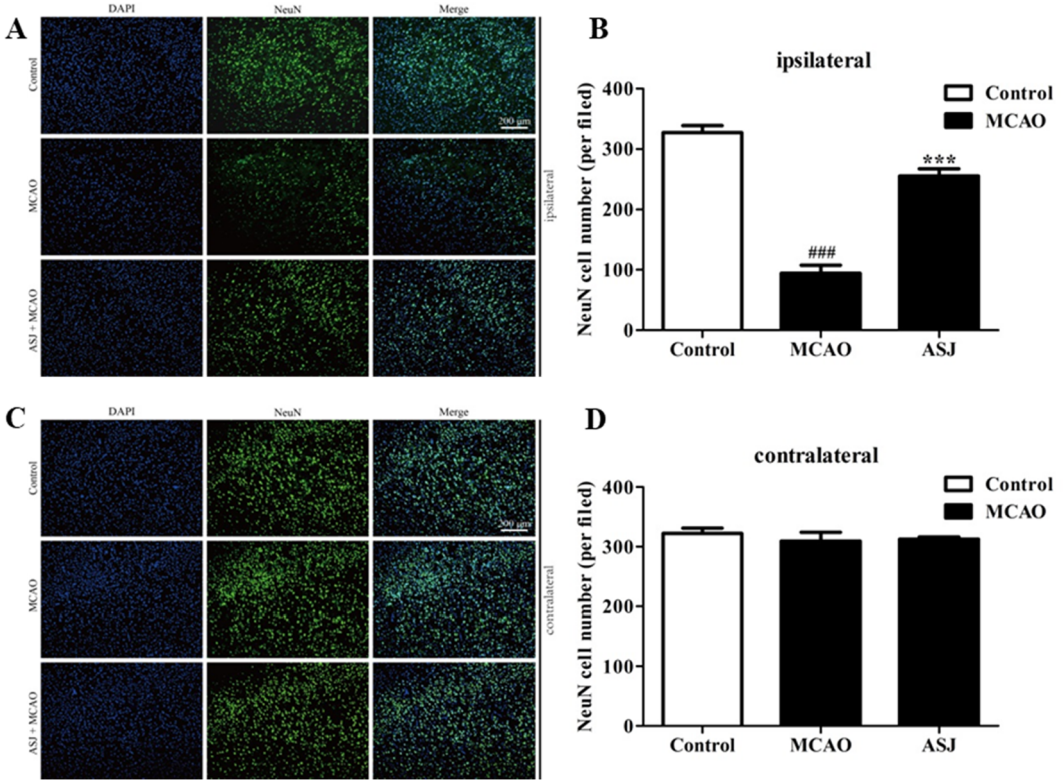

Fig. 8. Effect of ASJ on the number of NeuN positive cells in ipsilateral (A and B) and contralateral (C and D) cortex of MCAO rats at reperfusion 24 h. NeuN positive cells (green) in the ipsilateral cortex (A and B) were significantly reduced in the MCAO group compared with the control group. The reduction of mature neurons could be significantly inhibited by ASJ (200 mg/kg). NeuN positive cells (green) in the contralateral cortex (C and D) showed no significant difference between the groups. Values were expressed as Mean ± S.E.M, $###p < 0.001$ compared with the control group, $***p < 0.001$ compared with the MCAO group.

229.0 (−7.95), 219.0 (7.64); HRESIMS *m/z* $[M+H]^+$: 542.2390 (calcd. 542.2385 for $C_{29}H_{36}NO_9$); ^1H and ^{13}C NMR data were showed in Tables 1 and 2.

Stephalonine P (**5**), white powder (MeOH), $[\alpha]_D^{20}$ 5.76 (*c* 0.1, CH_3OH), λ_{max} (Δε) 293.0 (6.96), 273.0 (−38.01), 233.0 (39.45), 194.0 (−17.45); HRESIMS *m/z* $[M+H]^+$: 522.2492 (calcd. 522.2486 for $C_{30}H_{36}NO_7$); ^1H and ^{13}C NMR data were showed in Tables 1 and 2.

4.4. Single crystal X-ray diffraction analysis and crystallographic data of stephalonine L (1)

A crystal of **1** was selected for X-ray diffraction experiment. The X-ray diffraction measurements of compound **1** were made on a SuperNova, Dual, Cu at zero, AtlasS2 diffractometer with graphite-monochromated Cu Kα radiation. Crystal data: $C_{31}H_{39}NO_{11}$, Mr = 601.63, space group P $2_12_12_1$, a = 10.3061 (2) Å, b = 16.1624 (3) Å, c = 17.3401 (3) Å, α = 90, β = 90, γ = 90, V = 2888.36(9) $Å^3$, Z = 4, T = 100.01(10) K, μ (Cu Kα) = 0.877 mm^{-1}, F (0 0 0) = 1280.0, T = 293 K, 12,302 reflections were measured. The structure was solved with the ShelXT and refined with the ShelXL refinement package using Least Squares minimisation. *R*1 = 0.0387, w*R*2 = 0.1024 (all data). The crystallographic data for the structure of **1** have been deposited with the Cambridge Crystallographic Data Centre as supplementary publication CCDC No. 1935374.

4.5. Determination of cell viability.

BV2 cells were plated into 96-well plates at a concentration of 0.2×10^5 cells/mL. In the presence of LPS (100 ng/mL), the cells were pretreated with all test compounds in various concentrations (1, 10, 30 and 100 μM) for 24 h. After removing the culture supernatant, the cells were treated with 0.25 mg/mL of MTT for incubation for 3 h at 37 °C. Then, the absorbance of each well was recorded on a plate reader (Bio-Tek, Winooski, VT, USA) at 490 nm [20].

4.6. NO production bioassay.

Accumulation of NO_2^- was measured using the Griess reaction in culture medium. At concentration of 0.2×10^5 cells/well, BV2 cells were inoculated on 96-well microtiter plates and dealed with each isolate (1, 3, 10, 30, and 100 μM) in the presence of LPS (100 ng/mL) for 24 h [21]. Fifty microliter culture medium supernatants fluids were mixed with equivalent Griess reagent at room temperature, and measured their absorbance at 540 nm fifteen minutes later [22].

4.7. In vivo assessment of the effects of ASJ on MCAO rats

4.7.1. Animals and surgical procedure

Male Sprague-Dawley (SD) rats weighing 280–300 g were provided by Experimental Animal Center of Shenyang Pharmaceutical University (Shenyang, China) and were housed in room temperature environment under a 12 h light/dark cycle and allowed free access to food and water. All animal experiments followed the Regulations of Experimental Animal Administration issued by the State Committee of Science and Technology of the People's Republic of China.

MCAO was carried out as previously reported with some modifications [23]. In short, rats were anesthetized and a 4-0 monofilament nylon suture (4 mm silicon coating length, 0.26–0.28 mm tip diameter) was inserted into the middle cerebral arteries (MCA). After 1 h of MCAO, the monofilament was carefully removed to restore blood flow (reperfusion). MCAO was followed by reperfusion for 24 h.

4.7.2. Drug administration

The animals were grouped according to the random principle and

divided into 4 groups: the control group, the MCAO group, the ASJ treated group (100 and 200 mg/kg). After MCAO, the ASJ-treated group were immediately administrated with two doses at 100 mg/kg or 200 mg/kg by gavage. ASJ was dissolved in 0.5% carboxymethylcellulose sodium (CMC-Na), and rats in the control group and MCAO group were administered an equal volume of 0.5% CMC-Na.

4.7.3. Zea Longa neurological score

Neurological deficit scores were obtained after ischemic 1 h and at 24 h post- reperfusion. Our standard scoring system was as follows: 0, no deficit; 1, mild focal neurological deficit, lifting up the tail can't stretch the left fore paw; 2, moderate focal neurological deficit and turn left; 3, circling to affected side; 4, can't walk spontaneously or barrel rolling.

4.7.4. Measurement of cerebral infarction area

24 h after reperfusion, mice were anesthetized and brains were removed. Five serial sections from each brain were cut at 5 mm intervals. Sections were incubated in 1% 2,3,5-triphenyletrazolium chloride (TTC). Those areas were photographed and quantified with ImageJ image processing software (US National Institutes of Health, Bethesda, MD, USA) [24].

4.7.5. Tissue preparation

At 24 h after MCA occlusion and reperfusion, ischemic animals were deeply anesthetized and brain were harvested by decapitated. The brain is quickly frozen in liquid nitrogen and then stored in a −80 °C until used.

4.7.6. Immunofluorescence and analysis

The rat brains were sectioned by using a freezing microtome (LEICA CM1850) at a thickness of 10 μm for immunohistochemistry. The sections were blocked with normal goat serum (5% in 0.01 M PBS) for 30 min at room temperature, and then incubated with monoclonal rabbit Anti-Iba1 primary antibody (1:1000), rabbit anti-NeuN antibody (1:1000) for overnight at 4 °C. On the second day, sections were incubated with the Goat Anti-Rabbit IgG (FITC) for 60 min at 37 °C. Finally, sections were washed 3 times in PBS and coverslipped with Antifade Reagent (contain DAPI).

4.7.7. Reagents

ASJ was produced by our laboratory list in Section 4.3.

2,3,5-Triphenyltetrazolium chloride (TTC) was from Tianjin Damao Chemical Reagent Factory (Tianjin, China). Monoclonal anti-Iba1 antibody and monoclonal anti-NeuN antibody were from abcam (Cambridge, UK). Other chemicals and solvents in this experiment were all of analytical grade or higher.

4.7.8. Statistical analysis

Statistical analysis was conducted using SPSS 17.0 software (SPSS Inc., Chicago, IL, USA). Data were presented as mean ± SEM. One-way Analysis of Variance was used to evaluate the overall difference, followed by Least Significant Difference (LSD) or Dunnett's T3.

4.8. ECD calculation

All structures were established by Schrodinger 2013 package. Conformational searches were performed using the bioactive search function of conformational search protocol of the Schrodinger 2013 package with maximum 50 conformers. The conformers generated from conformational search were optimized at the B3LYP/6-311 + + G(2d, p) level using Gaussian09 package. The optimized conformers were aligned using the flexible ligand alignment protocol to examine if there were identical conformers for some structurally similar conformers would lead to the totally identical conformer after structure optimization. After merging the identical conformers, the remaining conformers were subjected to frequent analysis at the B3LYP/6-31G(d) level. Then all the conformers were subject to TD-DFT calculation of 50 states at the B3LYP/6-311 + + G(2d, p) level using Gaussian09 to generate ECD. All of the predominant conformers were optimized by DFT calculation at B3LYP/6-311 + + G(2d, p) level with the PCM in MeOH.

Acknowledgements

This work was financially supported by National Natural Science Foundation of China (Grant Nos. 81872768, 81673323, 81473108, U1603125, 81473330); LiaoNing Revitalization Talents Program (XLYC1807118), Liaoning BaiQianWan Talents Program (2018); Laboratory for Marine Drugs and Bioproducts of Qingdao National Laboratory for Marine Science and Technology (LMDBKF201701); The young and middle-aged teachers' career development support plan of Shenyang Pharmaceutical University; the Fundamental Research Funds for the Central Universities of China (N182008004, N182006001).

References

[1] M.S. Spychala, P. Honarpisheh, L.D. McCullough, Sex differences in neuroinflammation and neuroprotection in ischemic stroke, J. Neurosci. Res. 95 (2017) 462–471.
[2] A.K. Boehme, J.E. Siegler, M.T. Mullen, K.C. Albright, M.J. Lyerly, D.J. Monlezun, E.M. Jones, R. Tanner, N.R. Gonzales, T.M. Beasley, J.C. Grotta, S.I. Savitz, S. Martin-Schild, Racial and gender differences in stroke severity, outcomes, and treatment in patients with acute ischemic stroke, J. Stroke Cerebrovasc. Dis. 23 (2014) e255–e261.
[3] D. Mozaffarian, E.J. Benjamin, A.S. Go, D.K. Arnett, M.J. Blaha, M. Cushman, S.R. Das, S. de Ferranti, J.P. Despres, H.J. Fullerton, V.J. Howard, M.D. Huffman, C.R. Isasi, M.C. Jimenez, S.E. Judd, B.M. Kissela, J.H. Lichtman, L.D. Lisabeth, S. Liu, R.H. Mackey, D.J. Magid, D.K. McGuire, E.R. Mohler 3rd, C.S. Moy, P. Muntner, M.E. Mussolino, K. Nasir, R.W. Neumar, G. Nichol, L. Palaniappan, D.K. Pandey, M.J. Reeves, C.J. Rodriguez, W. Rosamond, P.D. Sorlie, J. Stein, A. Towfighi, T.N. Turan, S.S. Virani, D. Woo, R.W. Yeh, M.B. Turner, Heart disease and stroke statistics-2016 update: a report from the american heart association, Circulation 133 (2016) e38–e360.
[4] C. Iadecola, J. Anrather, The immunology of stroke: from mechanisms to translation, Nat. Med. 17 (2011) 796–808.
[5] H.C. Emsley, S.J. Hopkins, Acute ischaemic stroke and infection: recent and emerging concepts, Lancet Neurol. 7 (2008) 341–353.
[6] B.W. McColl, S.M. Allan, N.J. Rothwell, Systemic infection, inflammation and acute ischemic stroke, Neuroscience 158 (2009) 1049–1061.
[7] G. Yilmaz, D.N. Granger, Cell adhesion molecules and ischemic stroke, Neurol. Res. 30 (2008) 783–793.
[8] K.E. Hawkins, K.M. DeMars, J.C. Alexander, L.G. de Leon, S.C. Pacheco, C. Graves, C. Yang, A.O. McCrea, J.C. Frankowski, T.J. Garrett, M. Febo, E. Candelario-Jalil, Targeting resolution of neuroinflammation after ischemic stroke with a lipoxin A_4 analog: protective mechanisms and long-term effects on neurological recovery, Brain Behav. 7 (2017) e00688.
[9] J.Z. Deng, S.X. Zhao, Alkaloids from aerial parts of Stephania longa, Phytochemistry 33 (1993) 941–942.
[10] H. Zhang, J.M. Yue, Hasubanan type alkaloids from Stephania longa, J. Nat. Prod. 68 (2005) 1201–1207.
[11] M. Matsui, Y. Watanabe, T. Ibuka, K. Tanaka, Constitution of four new hasubanan alkaloids from Stephania japonica Miers, Tetrahedron Lett. 14 (1973) 4263–4266.
[12] M. Matsui, Y. Watanabe, T. Hinomoto, Carbon-13 NMR spectra of some hasubanan alkaloids, J. Nat. Prod. 45 (1982) 247–251.
[13] L. Tang, Y. Zhang, X. Hao, L. He, S. Song, X. Hao, X. Yang, Hasubanan type alkaloids in Stephania hernandifolia, Zhongguo Zhong Yao Za Zhi 35 (2010) 1973–1977.
[14] J.Y. Li, N. Li, X.Z. Li, G. Chen, C.G. Wang, B. Lin, Y. Hou, Characteristic alpha-acid derivatives from Humulus lupulus with Antineuroinflammatory activities, J. Nat. Prod. 80 (2017) 3081–3092.
[15] G.P. Moiseeva, S.Kh. Maekh, S. Yunusov, Circular dichroism of some bisbenzyltetrahydroisoquinoline alkaloids, Chem. Nat. Compd. 15 (1979) 723–727.
[16] Z.F. Guo, X.B. Wang, J.G. Luo, J. Luo, J.S. Wang, L.Y. Kong, A novel aporphine alkaloid from Magnolia officinalis, Fitoterapia 82 (2011) 637–641.
[17] P.L. Schiff, Bisbenzylisoquinoline alkaloids, J. Nat. Prod. 50 (1987) 529–599.
[18] M. Ropi Mukhtar, A. Zahari, M. Nafiah, A. Hamid, A. Hadi, N. Thomas, H. Arai, H. Morita, M. Litaudon, K. Awang, 3′, 4′-dihydronorstephasubine, a new bisbenzylisoquinoline from the bark of Alseodaphne corneri, Heterocycles 78 (2009) 2571–2578.
[19] S.V. Rabêlo, E.V. Costa, A. Barison, L.M. Dutra, X.P. Nunes, J.C. Tomaz, G.G. Oliveira, N.P. Lopes, M.d.F.C. Santos, J.R.G. da Silva Almeida, Alkaloids isolated from the leaves of atemoya (Annona cherimola Annona squamosa), Rev. Bras. Farmacog. 25 (2015) 419–421.
[20] Y. Hou, N. Li, G.B. Xie, J. Wang, Q. Yuan, C.G. Jia, X. Liu, G.X. Li, Y.Z. Tang, B. Wang, Pterostilbene exerts anti-neuroinflammatory effect on lipopolysaccharide-activated microglia via inhibition of MAPK signalling pathways, J. Funct. Foods 19 (2015) 676–687.

[21] Y. Song, L. Pan, W.J. Li, Y.Y. Si, D. Zhou, C.J. Zheng, X.F. Hao, X.Y. Jia, Y.M. Jia, M.H. Shi, X.G. Jia, N. Li, Y. Hou, Natural neuro-inflammatory inhibitors from Caragana turfanensis, Bioorg. Med. Chem. Lett. 27 (2017) 4765–4769.
[22] N. Li, Y. Wang, X.Z. Li, H. Zhang, D. Zhou, W.L. Wang, W. Li, X.R. Zhang, X.Y. Li, Y. Hou, D. Meng, Bioactive phenols as potential neuroinflammation inhibitors from the leaves of Xanthoceras sorbifolia Bunge, Bioorg. Med. Chem. Lett. 26 (2016) 5018–5023.
[23] F. Liu, L.D. McCullough, Inflammatory responses in hypoxic ischemic encephalopathy, Acta Pharmacol. Sin. 34 (2013) 1121–1130.
[24] Y. Suzuki, K. Hattori, J. Hamanaka, T. Murase, Y. Egashira, K. Mishiro, M. Ishiguro, K. Tsuruma, Y. Hirose, H. Tanaka, S. Yoshimura, M. Shimazawa, N. Inagaki, H. Nagasawa, T. Iwama, H. Hara, Pharmacological inhibition of TLR4-NOX4 signal protects against neuronal death in transient focal ischemia, Sci. Rep. 2 (2012) 896.